Functionalizing self-assembled GaN quantum dot superlattices by Eu-implantation

S. Magalhães,[1,2] M. Peres,[2] V. Fellmann,[3] B. Daudin,[3] A. J. Neves,[2] E. Alves,[1,4] T. Monteiro,[2] and K. Lorenz[1,4,a)]

[1]*Instituto Tecnológico e Nuclear, Estrada Nacional 10, 2685-953 Sacavém, Portugal*
[2]*Departamento de Física and i3N, Universidade de Aveiro, Campus de Santiago, 3810-193 Aveiro, Portugal*
[3]*Dépt. de Recherche Fondamentale sur la Matière Condensée, CEA/CNRS Group, "Nanophysique et Semiconducteurs," CEA/Grenoble, 17 rue des Martyrs, 38054 Grenoble Cedex 9, France*
[4]*CFNUL, Av. Prof. Gama Pinto, 1649-003 Lisboa, Portugal*

(Received 22 July 2010; accepted 27 August 2010; published online 21 October 2010)

Self-assembled GaN quantum dots (QDs) stacked in superlattices (SL) with AlN spacer layers were implanted with Europium ions to fluences of 10^{13}, 10^{14}, and 10^{15} cm^{-2}. The damage level introduced in the QDs by the implantation stays well below that of thick GaN epilayers. For the lowest fluence, the structural properties remain unchanged after implantation and annealing while for higher fluences the implantation damage causes an expansion of the SL in the [0001] direction which increases with implantation fluence and is only partly reversed after thermal annealing at 1000 °C. Nevertheless, in all cases, the SL quality remains very good after implantation and annealing with Eu ions incorporated preferentially into near-substitutional cation sites. Eu^{3+} optical activation is achieved after annealing in all samples. In the sample implanted with the lowest fluence, the Eu^{3+} emission arises mainly from Eu incorporated inside the QDs while for the higher fluences only the emission from Eu inside the AlN-buffer, capping, and spacer layers is observed.
 [doi:10.1063/1.3496624]

I. INTRODUCTION

Functionalizing group III nitride semiconductors by doping with rare earth (RE) ions leads to light emission in the infrared, visible, and ultraviolet spectral regions due to intraionic transitions within the trivalent RE^{3+} ions. Sharp red (Pr^{3+} and Eu^{3+}), green (Er^{3+} and Tb^{3+}), and blue (Tm^{3+}) emission lines have been observed from *in situ* doped[1] and ion-implanted[2] GaN opening the possibility to produce all-nitride full-color photonic devices. Eu-doping is of particular interest due to its intense red emission while conventional InGaN-based light emitting diodes (LEDs) have low efficiency in the green and red spectral regions. The low efficiency is a result of difficulties in growing high quality material with high InN contents of the InGaN active layers and problems caused by the quantum confined Stark effect in polar heterostructures.[3]

Recently, laser action in GaN:Eu upon optical pumping[4] and the first low-voltage operation of current-injected red emission from a GaN:Eu LED (Ref. 5) were demonstrated. However, the light emission efficiency is still low compared to conventional red LEDs. The main problem here lies in the inefficient energy transfer from the host semiconductor to the RE ions. Another issue is the low RE concentration which is limited by concentration quenching and specific problems of the different doping techniques: phase separations and deterioration of the crystal quality can occur in *in situ* doped material and strong radiation damage leads to nonradiative recombination centers in high-fluence ion-implanted samples. In order to increase the efficiency of RE emission it may be of advantage to dope GaN nanostructures like quantum dots (QDs). The carrier confinement inside the QDs can increase the excitation cross-section and the high crystal quality typically evidenced in GaN QDs decreases nonradiative de-excitation paths. Such an increase in RE^{3+} luminescence quantum efficiency was reported for Sm^{3+}-doped $ZnS_{0.8}Se_{0.2}$/undoped ZnS multiple-quantum wells[6] and the effect may be even enhanced for one-dimensional confinement in QDs. *In situ* doping of GaN QDs with RE ions during growth by molecular beam epitaxy (MBE) has been reported. Very temperature stable red emission was found for Eu-doped QD.[7] The incorporation of Tm inside QDs, on the other hand, was found to be difficult as it tends to be preferentially incorporated into the AlN spacer layers.[8,9] Furthermore, does the addition of RE during growth alter the growth kinetics influencing the two-dimensional/three-dimensional transition of the Stranski Krastanow process.[10] Ion implantation of pre-grown GaN QDs may circumvent these problems of RE incorporation. However, ion-implantation inevitably causes large amounts of defects which have to be removed by high temperature annealing in order to optically activate RE ions. Furthermore, in the case of implanted superlattices (SL) of thin semiconductor layers the implantation and the annealing can cause intermixing. Annealing of InGaN QDs for example resulted in the shrinkage of the QD size and eventually in the mergence of the QDs into the wetting layer leading to the loss of the one-dimensional confinement.[11]

In this work, we implanted Eu into a 20 period SL consisting of GaN QD and AlN spacer layers. The SL structure is well preserved after implantation/annealing and Eu is incorporated mainly into substitutional cation sites. Optical activation of the Eu^{3+} ions is achieved. For low fluences, the

a)Electronic mail: lorenz@itn.pt.

Eu^{3+} emission is mainly observed from ions located inside the GaN QDs while for higher fluences it is dominated by lines from Eu^{3+} ions incorporated into the AlN host.

II. EXPERIMENTAL DETAILS

A GaN QD/AlN SL sample (no. 989) was grown by MBE on a commercial 1×1 cm^2 AlN/sapphire pseudosubstrate grown by metal organic chemical vapor deposition. After standard cleaning of the pseudosubstrate a ~240 nm thick AlN-buffer layer was grown followed by a 20 periods SL consisting of GaN QD planes grown at 740 °C by the Stranski Krastanow growth mode and separated by AlN spacer layers. A detailed description of the growth process has been reported in Ref. 12. The size and density of the QDs are controlled by the GaN deposition time which was 18 s (corresponding to ~6 monolayers) leading typically to QD heights and densities of ~5 nm and 2×10^{11} cm^{-2}, respectively.[12] Finally, the sample was capped by a ~40 nm AlN layer. It was shown before that a thin AlN capping layer on GaN films as well as GaN QDs effectively protects the GaN from dissociation during high temperature post-implant annealing.[13,14]

Subsequently, the sample was cut into three pieces and implanted with 300 keV Eu ions to fluences of 1×10^{13}, 1×10^{14}, and 1×10^{15} cm^{-2}. The implantation was performed at room temperature and with the beam aligned with the *c*-axis of the samples since this channeled geometry was shown to considerably decrease the implantation damage in GaN and AlN thin films.[15,16]

Post-implant annealing to remove implantation damage and optically activate the Eu ions was performed at 1000 °C in flowing N_2 at 1 bar pressure and placing a piece of AlN/sapphire face to face with the samples as a proximity cap to protect the surface during the high temperature treatment.

An additional sample (no. 987) with similar growth conditions and implanted to a fluence of 1×10^{15} cm^{-2} was prepared to perform high resolution X-ray diffraction (HR-XRD) reciprocal space mapping (RSM).

HR-XRD was performed using monochromated Cu $K_{\alpha1}$ radiation on a D8-Discover system from Bruker-AXS using a Göbel mirror, an asymmetric 2-bounce Ge(220) monochromator and a scintillation detector.

Rutherford backscattering spectrometry and channeling (RBS/C) measurements with 2 MeV He^+ particles, a two axes goniometer and two Si surface barrier detectors at ~180° and 140° backscattering angle were used to assess the implantation damage in GaN QD and AlN spacer layers and the Eu incorporation and profile. Full angular scans were fitted with help of the Monte Carlo code FLUX.[17] Since FLUX does not take into account any defects that may cause a static displacement of the atoms which leads to a narrowing of channeling dips, such a displacement was fitted by increasing the vibration amplitude of the atoms in the simulation.

Photoluminescence (PL) measurements were carried out with the 325 nm line of a cw He–Cd laser and PL excitation (PLE) by a 1000 W Xe lamp coupled to a monochromator. All the spectra were corrected to the efficiencies of lamp and optics.

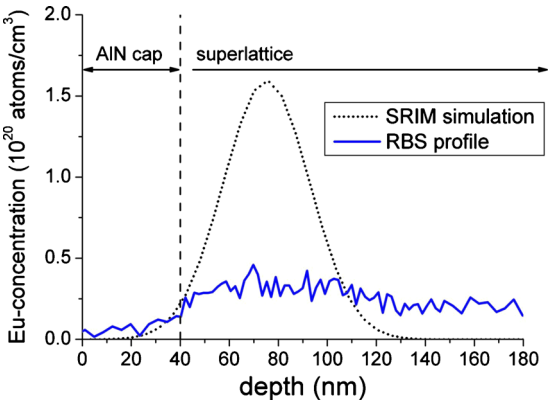

FIG. 1. (Color online) Experimental and simulated (SRIM2008) Eu-depth profiles after implantation of 1×10^{15} cm^{-2} at 300 keV into a 20-period GaN QD/AlN SL with ~9.5 nm period thickness and ~40 nm AlN capping layer.

III. RESULTS AND DISCUSSION

A. Structural analysis

Figure 1 shows the Eu-profile measured by RBS together with the profile derived from SRIM2008 (Ref. 18) simulations.

The measured profile reaches deeper into the sample than predicted by the simulation due to strong channeling effects that occur when the implantation is performed along the *c*-axis of the sample and which are not taken into account in the simulations. The Eu ions are distributed within the entire SL region and possibly reach the AlN-buffer layer (the RBS results are not conclusive at this depth due to the starting overlap of the signals from Eu and Ga).

X-ray reflection (XRR) profiles of the as-grown samples have been published previously;[19] the derived period thickness for both samples discussed here is 9.5(2) nm and does not change with implantation or annealing. The high number of visible SL peaks in XRR specular curves[19] and XRD $2\theta-\omega$ scans (up to order 6, see Fig. 2) reveal an excellent quality of layers and interfaces.

Figure 2 presents XRD $2\theta-\omega$ scans of the 002 reflection for the as-grown sample no. 989 and the implanted samples before and after annealing at 1000 °C.

In all scans, the 002 reflection of the AlN-buffer layer is visible together with several SL peaks. From the position of the SL0 peak, the average *c*-lattice constant of the SL can be determined. For the as-grown sample, this average *c*-parameter is 5.007(2) Å from which the average GaN content is estimated to be ~10% assuming that the GaN QD and AlN spacer layers are grown coherently on the AlN-buffer layer, consistent with the nominal sample structure. After implantation a shift in the SL0 peak to smaller angles (higher average SL *c*-parameters) is observed for the two higher fluences. The average SL *c*-lattice parameter after implantation with the lowest fluence does not change but then increases gradually with implantation fluence as seen in Fig. 3; for the highest fluence it increases by ~1%. Such expansion of the lattice due to implantation defects is known to occur upon implantation or irradiation of thick GaN (Refs. 20 and 21) and AlN films as well as their alloys.[22]

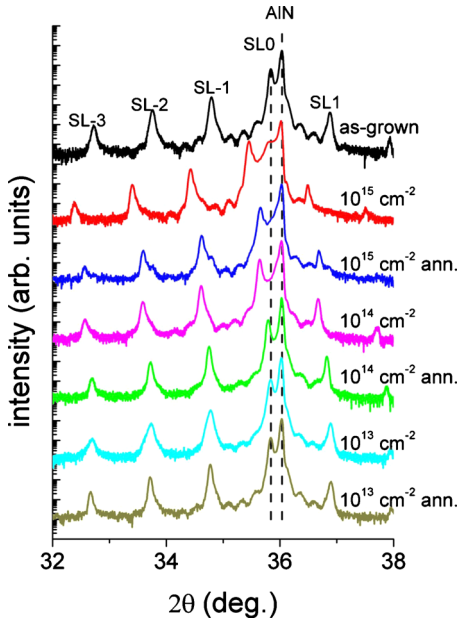

FIG. 2. (Color online) $2\theta-\omega$ scans of the symmetric 002 reflection of the as-grown SL sample no. 989 and the as-implanted and annealed (ann.) samples for different implantation fluences.

After annealing at 1000 °C, the SL0 peak shifts back towards the position of the as-grown sample. However, only partial recovery of the crystal is observed for fluences of 1×10^{14} and 1×10^{15} cm^{-2}; for the annealing temperatures used here not all defects can be removed and the SL0 peaks do not reach the value of the as-grown sample (Fig. 3).

It is worth mentioning that annealing the as-grown samples leaves the (002) $2\theta-\omega$ scans unchanged and only small alterations are seen in the XRR curves indicating some modification of the interfaces while large shifts in the QD emission wavelengths have been observed, attributed to the balance between the quantum confinement and quantum confined Stark effect altered due to interdiffusion and/or local strain relaxation processes.[19]

The symmetric $2\theta-\omega$ scans discussed so far only give information on the *c*-lattice parameter. In order to investigate if the implantation also affects the average *a*-lattice parameter of the SL, RSMs around the 105 asymmetric reciprocal lattice point were acquired for sample no. 987 in the as-grown state, after implantation and after annealing (Fig. 4).

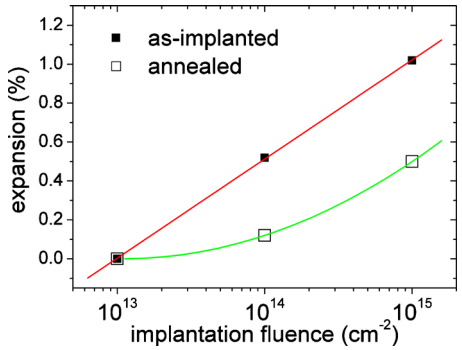

FIG. 3. (Color online) The relative expansion of the average *c*-parameter of the SL as a function of the implantation fluence. The lines are a guide to the eye.

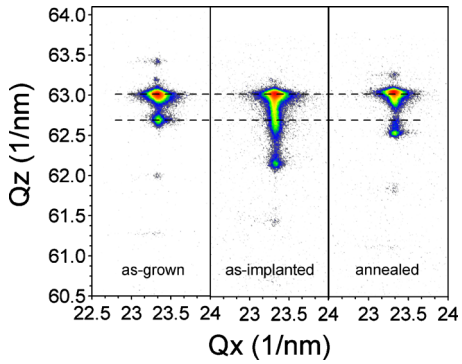

FIG. 4. (Color online) Asymmetric RSM around the 105 reciprocal lattice point of the as-grown, the as-implanted (1×10^{15} cm^{-2} at 300 keV) and the implanted and annealed SL sample no. 987.

The reflections of AlN and the SL0 peak lie on a vertical line confirming that the SL is growing coherently on the AlN-buffer layer. The effect of the expected strain relaxation within the as-grown GaN QDs is too small to be measured here.

The RSM after implantation clearly shows a shift in the SL0 peak to smaller Qz values while the Qx value stays the same proving that the *a*-lattice parameter remains unchanged after implantation and only the *c*-lattice parameter increases. The elongation of the AlN 105 reflection to lower Qz values is caused by the implantation damage in the AlN-buffer layer as a fraction of Eu ions cross the SL region and reach the buffer layer, leading to an expansion of the *c*-lattice parameter in this region.

Figure 5 shows random and aligned RBS/C spectra of sample no. 989 before and after implantation with 1×10^{15} cm^{-2}.

The fit to the random spectrum was performed using the NDF code[23] and allows the determination of the Eu-profile (Fig. 1) and an estimation of the average GaN content in the SL which is ~10% in good agreement with the value estimated from the XRD data. The Ga minimum yield χ_{min}(Ga) (backscattering yield of the aligned spectrum divided by the yield of the random spectrum) corresponding to the GaN QDs is found to be 2.5% in the as-grown sample confirming

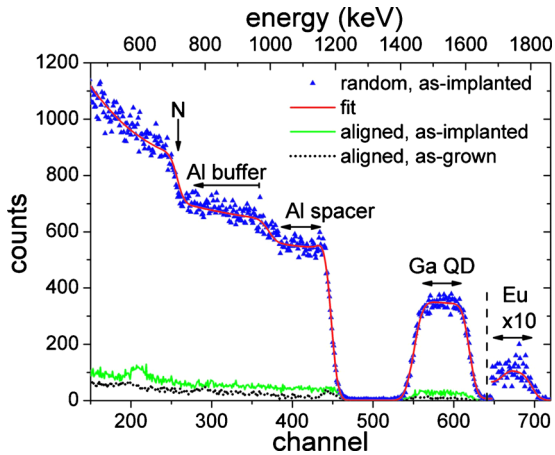

FIG. 5. (Color online) Random and ⟨0001⟩ aligned RBS/C spectra of the as-grown and the as-implanted (1×10^{15} cm^{-2} at 300 keV) SL sample no. 989.

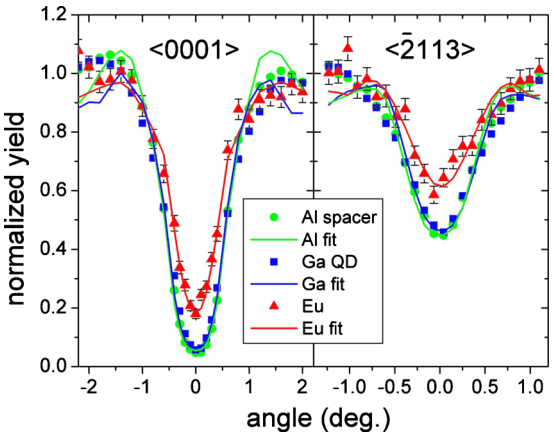

FIG. 6. (Color online) Full angular RBS/C scans across the ⟨0001⟩ and ⟨$\bar{2}$113⟩ crystal axes of the implanted (1×10^{15} cm^{-2} at 300 keV) and annealed SL sample no. 989. The scans are almost identical to those directly after implantation. The used depth windows for Eu, Ga (from the GaN QD), and Al (from the AlN spacer layers) are indicated in Fig. 5.

the good single crystalline quality of the sample comparable to thick state-of-the-art GaN epilayers.[21] After implantation χ_{min}(Ga) increases slightly to 8%. A GaN layer implanted simultaneously, on the other hand, showed a strong increase in the minimum yield after implantation from 2% to 16%. These results reveal a remarkable radiation hardness of GaN QDs compared to GaN epitaxial layers.[24] The minimum yield in a window comprising the AlN spacer layers was found to be comparable to both that of the GaN QDs and that of a thick AlN layer implanted in the same conditions. Annealing at 1000 °C partly removes implantation damage and reduces the minimum yield to χ_{min}(Ga)=5%.

The incorporation of Eu in the SL was investigated by performing full angular scans across the ⟨0001⟩ and ⟨$\bar{2}$113⟩ axes for the sample implanted to the highest fluence (Fig. 6).

Depth windows were chosen for Al (corresponding to the AlN spacer layers), Ga (corresponding to GaN QDs) and Eu (corresponding to the entire implanted region) as indicated in Fig. 5. While the scans for Ga and Al overlap, it is clearly seen that the scans for Eu are narrower for the two crystal directions, indicating that Eu is incorporated slightly displaced from the substitutional cation-site. The same is also observed for Eu-implanted GaN and AlN films prepared under similar conditions.[25,26] The fits to the experimental scans are also shown in Fig. 6 and used vibration amplitudes of 0.18(2) Å, 0.20(2) Å, and 0.28(2) Å for Al, Ga, and Eu, respectively, for the ⟨0001⟩ direction, and 0.21(2) Å, 0.24(2) Å, and 0.4(1) Å for the ⟨$\bar{2}$113⟩ direction. The values for Al and Ga are significantly higher than literature values for bulk GaN (0.1 Å) (Ref. 27) and AlN (0.08 Å) (Ref. 28) hinting to a static displacement due to defects and lattice mismatch between the different layers. The increased values derived for Eu give an estimate of its displacement from the substitutional site. However, the dip for the tilted direction is not well defined not allowing an accurate determination of the magnitude nor the exact direction of the displacement. Nevertheless, both scan directions confirm a displacement from the substitutional site. The near-substitutional fraction was estimated to be 84% directly after the implantation. Both the substitutional fraction and the displacement remained unchanged after annealing. Naturally, Eu is incorporated into GaN QD as well as AlN layers and from these measurements it is not possible to distinguish both incorporation sites.

B. Optical analysis

Assuming that the Eu fraction incorporated into GaN QDs corresponds in first estimation to the average GaN content in the SL, only ~10% of the implanted Eu ions actually come to rest inside the QDs and the remaining 90% are incorporated into AlN spacer, capping, and buffer layers. Since Eu^{3+} is optically active in both matrixes the intraionic luminescence may arise from both Eu^{3+} inside GaN QD and within the AlN host. Additionally, implantation and annealing may cause intermixing of the layers in the SL leading to regions with compositional gradients and properties of ternary $Al_xGa_{1-x}N$ alloys. Therefore, the identification of the different incorporation sites and optically active centers of Eu^{3+} in the QD SL samples requires the comparison with Eu^{3+} emissions from GaN, AlN, and $Al_xGa_{1-x}N$ material.

The most intense luminescence of Eu^{3+} in these nitride hosts is known to arise from the $^5D_0\rightarrow{}^7F_2$ transition which occurs at ~624 nm in the AlN host and is blueshifted in GaN by ~2.2 nm.[29,30] Furthermore, Eu^{3+} ions are known to give rise to multiple active centers in the binary systems.[31,32] In this context, it is important to emphasize the difference of the lattice site location of Eu (Eu is known to be incorporated into near-substitutional Ga and Al sites in GaN and AlN, respectively[25,26]) and the different optically active centers (often also called "sites") which depend on the local symmetry around the substitutional Eu (which can for example be influenced by next neighbor defects).

Figure 7 presents the PL spectra showing the main $^5D_0\rightarrow{}^7F_2$ transition excited using the 325 nm laser line of all SL samples as well as GaN, AlN, and $Al_{0.5}Ga_{0.5}N$ epilayers implanted with 1×10^{15} cm^{-2} and annealed.

This excitation energy lies above the band gap of the GaN QDs but below that of AlN. Nevertheless, it is well known that broad absorption bands below the band gap of AlN and AlGaN alloys allow the excitation of Eu^{3+} at this wavelength.[29] All the implanted and annealed SL and epilayer samples evidence Eu^{3+} emission in the red spectral region. The PL intensity of the SL samples increases with the implantation fluence. Besides the Eu^{3+} emission all SL samples also maintain their excitonic QD emission (not shown) at ~450 nm which is slightly blueshifted compared to the as-grown sample consistent with an earlier study of annealed QDs.[19]

For the two higher implantation fluences, in the ion-implanted and annealed SL, the peak position of the $^5D_0\rightarrow{}^7F_2$ transition occurs around 624 nm. Three sharp but partially overlapping lines can be distinguished and a direct comparison with the spectrum of the AlN:Eu layer indicates that the Eu^{3+} emission in the SL samples implanted with 1×10^{14} and 1×10^{15} cm^{-2} arises mainly from the AlN host (buffer, spacer or capping layers). Only slight changes in the lines' relative intensities are seen while the peak positions are exactly the same as for AlN:Eu.

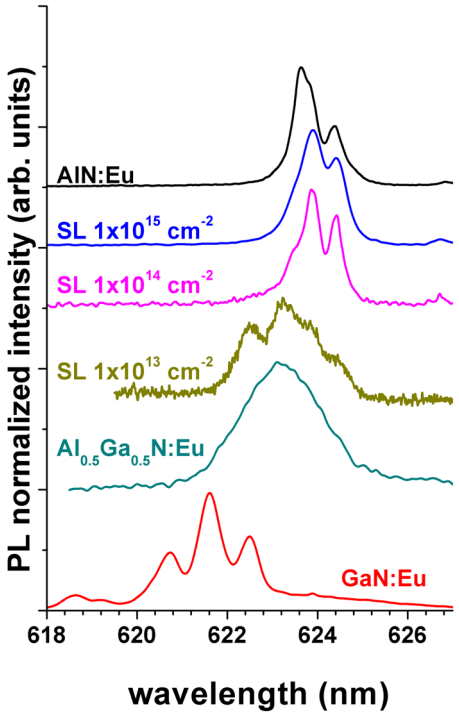

FIG. 7. (Color online) 14 K PL spectra (excited with the 325 nm laser line) in the different ion-implanted and annealed samples. The implantation fluence of all the epilayer samples was 1×10^{15} cm^{-2}.

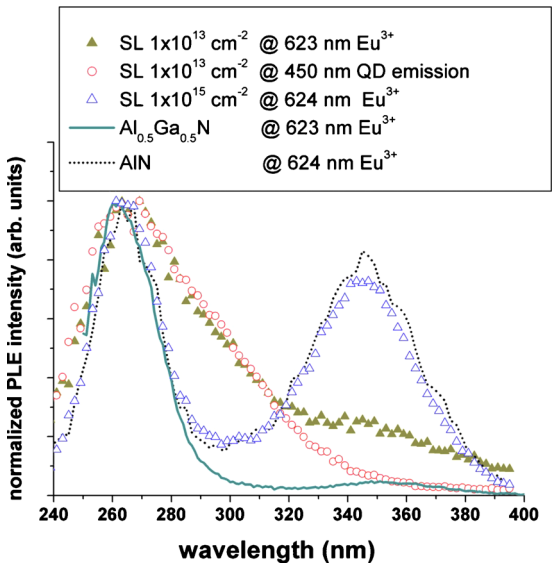

FIG. 8. (Color online) 14 K PLE spectra of the SL samples no. 989 implanted to 1×10^{13} and 1×10^{15} cm^{-2} monitored at the most intense $^5D_0\rightarrow{}^7F_2$ Eu^{3+} emission line. For the low fluence SL the PLE spectrum monitored at the excitonic GaN QDs recombination is also presented. For comparison, the PLE spectra monitored at the Eu^{3+} luminescence for Eu-implanted $Al_{0.5}Ga_{0.5}N$ and AlN are also shown.

In contrast, for the sample implanted with lower fluence at least four Eu^{3+}-related lines are resolved, the more intense one peaked at 623.2 nm. The intensity of the emission is weak due to the low Eu concentration, however, it is clearly seen that the positions of the two lines at higher wavelengths correspond to those observed in the high-fluence sample (assigned to Eu^{3+} in AlN). The two lines at 622.5 and 623.2 nm do neither correspond to emissions of Eu^{3+} in AlN nor to the typical wavelength of Eu^{3+} emission from GaN that shows sharp emission lines around 620–623 nm. Nevertheless, the emission of Eu^{3+} inside QDs may be shifted due to the different strain state of GaN QDs grown on AlN-buffer layers compared to thick films grown on GaN buffer layers. On the other hand, does the observed wavelength of Eu^{3+} emission resemble that of Eu^{3+} implanted into $Al_xGa_{1-x}N$ with x $\sim$50% and the possibility that it may have its origin in some region that suffered intermixing during the implantation has to be investigated.

In order to discriminate between Eu centers in different host materials and to study the excitation transfer mechanisms, PLE spectra monitored at the highest $^5D_0\rightarrow{}^7F_2$ emission peak were taken (Fig. 8). The PLE spectrum of a SL sample monitored at the main excitonic QD emission around 450 nm is also shown.

All SL and AlN samples show intense absorption bands around 265 nm to which the PLE spectra are normalized. It is important to note that this band excites not only the Eu^{3+}-ions but also the QD excitonic emission. PLE on the Eu^{3+}-lines in AlN:Eu shows a second broad absorption band peaked at $\sim$345 nm. In AlN:Eu, these two bands were labeled as X_2 and X_1, respectively, by Wang *et al.*[29] and interpreted as excitonic features associated with a specific Eu^{3+} center. The observation of these two absorption bands in Eu-implanted AlN samples was also reported by other authors.[33] In the SL samples, the relative intensity of the X_1 absorption band is increasing with the Eu concentration and for the highest fluence the PLE spectrum is almost identical to that of the AlN:Eu layer which was implanted to the same fluence. The fact that both PL and PLE show identical features in AlN:Eu and the SL indicates that in the SL samples implanted to the two higher fluences the main optically active Eu center resides in the AlN host of the buffer, capping, and spacer layers.

For the SL sample implanted with the lowest fluence, the excitation band at 265 nm is asymmetrically broadened to higher wavelengths. In fact, the PLE spectrum monitoring the main Eu^{3+} line and the one monitoring the QD excitonic emission completely overlap for wavelengths below 320 nm. This behavior suggests that the Eu^{3+} emission in this sample is preferentially excited via the GaN QDs absorption band. Additionally, the PL peak position (Fig. 7) indicated that the dominant emitting Eu^{3+} ions must be located in GaN QDs while lines corresponding to AlN:Eu are weaker. In this sample, the $\sim$345 nm X_1 absorption band characteristic for Eu^{3+} in AlN:Eu layers is very weak and partially overlapped with the excited state absorption band of the GaN QDs. At 325 nm (the excitation wavelength used for the PL spectra in Fig. 7), it can be assumed that both Eu in QDs and Eu in AlN are being excited.

Although the absorption bands in the different hosts partly overlap the possibility of Eu incorporated into $Al_xGa_{1-x}N$ in areas of strong intermixing can furthermore be discarded by comparing the PLE spectra of $Al_xGa_{1-x}N$:Eu with those of the SL samples (Fig. 8). In $Al_{0.5}Ga_{0.5}N$, Eu^{3+} is excited via an absorption band around 265 nm that corresponds to the band gap of the $Al_{0.5}Ga_{0.5}N$ alloy and the X_1

band below the band gap around 350 nm. However, the absorption around 300 nm which excited Eu^{3+} as well as the QD excitonic emission in the SL sample is absent in this sample.

These results suggest that the dominant Eu^{3+} optically active center in the low fluence SL sample is associated to Eu incorporated inside the GaN QDs. This observation is particularly important having in mind that only ~10% of the Eu ions are actually incorporated into the GaN QDs while the majority resides in the AlN host. These results point to a more efficient excitation of Eu^{3+} inside the QD although the different excitation conditions for PL in QD and spacer layers (above the GaN band gap but below the AlN band gap) do not allow a quantitative analysis. The beneficial effect of quantum confinement is further confirmed by a low temperature quenching of the PL in this sample compared to that of thick GaN:Eu films.[34]

IV. CONCLUSIONS

Implanting Eu ions into GaN QD/AlN SL results in Eu incorporation into GaN QDs as well as into the AlN layers. After implantation and annealing Eu is found mainly on near-substitutional cation sites. Implantation to a low Eu fluence of 1×10^{13} cm^{-2} introduces negligible amounts of lattice damage and the dominant optically active Eu center found in this sample can be attributed to Eu incorporated into GaN QDs. Higher implantation fluences of 1×10^{14} and 1×10^{15} cm^{-2}, on the other hand, lead to higher lattice damage that provokes an expansion of the lattice that could only be partly removed by thermal annealing. This irreversible damage leads to a quenching of luminescence from Eu inside QDs and the main optically active center in these samples is attributed to Eu inside the AlN host in buffer, spacer, and capping layers.

ACKNOWLEDGMENTS

Funding by FCT Portugal (Ciência 2007 and Grant No. PTDC/CTM/100756/2008) and by the bilateral collaboration program PESSOA (EGIDE/GRICES) is gratefully acknowledged. M. Peres and S. Magalhães thank FCT for their grants, Grant Nos. SFRH/BD/45774/2008 and SFRH/BD/44635/2008, respectively. We thank N. Franco (ITN, Portugal) for the assistance with the XRD measurements.

[1]A. J. Steckl, J. C. Heikenfeld, D. S. Lee, M. J. Garter, C. C. Baker, Y. Wang, and R. Jones, IEEE J. Sel. Top. Quantum Electron. **8**, 749 (2002).
[2]H. J. Lozykowski, W. M. Jadwisienczak, and I. Brown, Appl. Phys. Lett. **74**, 1129 (1999).
[3]R. A. Oliver and B. Daudin, Philos. Mag. **87**, 1967 (2007) and references therein.
[4]A. J. Steckl, J. H. Park, and J. M. Zavada, Mater. Today **10**, 20 (2007).
[5]A. Nishikawa, T. Kawasaki, N. Furukawa, Y. Terai, and Y. Fujiwara, Appl. Phys. Express **2**, 071004 (2009).
[6]M. Tanaka, H. Yamada, T. Maruyama, and K. Akimoto, Phys. Rev. B **67**, 045305 (2003).
[7]Y. Hori, F. Enjalbert, E. Monroy, D. Jalabert, L. S. Dang, X. Biquard, M. Tanaka, O. Oda, and B. Daudin, Appl. Phys. Lett. **84**, 206 (2004).
[8]T. Andreev, Y. Hori, X. Biquard, E. Monroy, D. Jalabert, A. Farchi, M. Tanaka, O. Oda, L. S. Dang, and B. Daudin, Phys. Rev. B **71**, 115310 (2005).
[9]H. Okuno, J.-L. Rouvière, P.-H. Jouneau, P. Bayle-Guillemaud, and B. Daudin, Appl. Phys. Lett. **96**, 251908 (2010).
[10]Y. Hori, D. Jalabert, T. Andreev, E. Monroy, M. Tanaka, O. Oda, and B. Daudin, Appl. Phys. Lett. **84**, 2247 (2004).
[11]Q. Wang, T. Wang, J. Bai, A. G. Cullis, P. J. Parbrook, and F. Ranalli, Appl. Phys. Lett. **93**, 081915 (2008).
[12]C. Adelmann, B. Daudin, R. A. Oliver, G. A. D. Briggs, and R. E. Rudd, Phys. Rev. B **70**, 125427 (2004).
[13]K. Lorenz, U. Wahl, E. Alves, S. Dalmasso, R. W. Martin, K. P. O'Donnell, S. Ruffenach, and O. Briot, Appl. Phys. Lett. **85**, 2712 (2004).
[14]S. Magalhães, K. Lorenz, N. Franco, N. P. Barradas, E. Alves, T. Monteiro, B. Amstatt, V. Fellmann, and B. Daudin, Surf. Interface Anal. **42**, 1552 (2010).
[15]B. Pipeleers, S. M. Hogg, and A. Vantomme, J. Appl. Phys. **98**, 123504 (2005).
[16]K. Lorenz, E. Alves, F. Gloux, P. Ruterana, M. Peres, A. J. Neves, and T. Monteiro, J. Appl. Phys. **107**, 023525 (2010).
[17]P. J. M. Smulders and D. O. Boerma, Nucl. Instrum. Methods Phys. Res. B **29**, 471 (1987).
[18]J. F. Ziegler, J. P. Biersack, and U. Littmark, *The Stopping and Range of Ions in Solids* (Pergamon, New York, 1985).
[19]M. Peres, A. J. Neves, T. Monteiro, S. Magalhães, E. Alves, K. Lorenz, H. Okuno-Vila, V. Fellmann, C. Bougerol, and B. Daudin, Phys. Status Solidi B **247**, 1675 (2010).
[20]C. Liu, B. Mensching, K. Volz, and B. Rauschenbach, Appl. Phys. Lett. **71**, 2313 (1997).
[21]J. G. Marques, K. Lorenz, N. Franco, and E. Alves, Nucl. Instrum. Methods Phys. Res. B **249**, 358 (2006).
[22]M. Peres, S. Magalhães, N. Franco, M. J. Soares, A. J. Neves, E. Alves, K. Lorenz, and T. Monteiro, Microelectron. J. **40**, 377 (2009).
[23]N. P. Barradas, C. Jeynes, and R. P. Webb, Appl. Phys. Lett. **71**, 291 (1997).
[24]K. Lorenz, N. P. Barradas, E. Alves, I. S. Roqan, E. Nogales, R. W. Martin, K. P. O'Donnell, F. Gloux, and P. Ruterana, J. Phys. D: Appl. Phys. **42**, 165103 (2009).
[25]T. Monteiro, C. Boemare, M. J. Soares, R. A. S. Ferreira, L. D. Carlos, K. Lorenz, R. Vianden, and E. Alves, Physica B **308–310**, 22 (2001).
[26]M. Peres, A. Cruz, M. J. Soares, A. J. Neves, T. Monteiro, K. Lorenz, and E. Alves, Superlattices Microstruct. **40**, 537 (2006).
[27]A. Yoshiasa, K. Koto, H. Maeda, and T. Ishii, Jpn. J. Appl. Phys., Part 1 **36**, 781 (1997).
[28]E. Gabe, Y. L. Page, and S. L. Mair, Phys. Rev. B **24**, 5634 (1981).
[29]K. Wang, K. P. O'Donnell, B. Hourahine, R. W. Martin, I. M. Watson, K. Lorenz, and E. Alves, Phys. Rev. B **80**, 125206 (2009).
[30]M. Peres, A. J. Neves, T. Monteiro, S. Magalhães, N. Franco, K. Lorenz, E. Alves, B. Damilano, J. Massies, A. Dussaigne, and N. Grandjean, J. Nanosci. Nanotechnol. **10**, 2473 (2010).
[31]K. Wang, R. W. Martin, K. P. O'Donnell, V. Katchkanov, K. Lorenz, E. Alves, S. Ruffenach, and O. Briot, Appl. Phys. Lett. **87**, 112107 (2005).
[32]L. Bodiou, A. Braud, J.-L. Doualan, R. Moncorgé, J. H. Park, C. Munasinghe, A. J. Steckl, K. Lorenz, E. Alves, and B. Daudin, J. Appl. Phys. **105**, 043104 (2009).
[33]H. J. Lozykowski, W. M. Jadwisienczak, A. Bensaoula, and O. Monteiro, Microelectron. J. **36**, 453 (2005).
[34]M. Peres, S. Magalhães, J. Rodrigues, M. J. Soares, V. Fellmann, A. J. Neves, E. Alves, B. Daudin, K. Lorenz, and T. Monteiro, "The role of the annealing temperature on the optical and structural properties of Eu doped GaN/AlN QDs," Optical Materials (submitted).